THE ASSESSMENT OF DEFECTS UNDER MIXED MODE LOADING

P. J. Budden* and M. R. Jones+

Elastic-plastic crack growth under mixed Modes 1 and 2 small scale yielding conditions is addressed. Both brittle and ductile failure micromechanisms are considered. The relationship between the applied stress intensity factors at fracture is discussed and an effective stress intensity factor for mixed Modes 1 and 2 loading is defined. This definition is used with the R6 defect assessment procedure to examine mixed mode specimen failure data and is shown to be consistent with most of the data.

INTRODUCTION

The R6 procedure (Milne et al, (1)) for the assessment of defective structures operating in the elastic-plastic fracture regime is well-developed and validated for Mode 1 loading. R6 considers the two extremes of material behaviour, brittle fracture and plastic collapse, and interpolates between the two on a Failure Assessment Diagram. Mixed mode loading is addressed by either suitably recharacterizing the defect such that the loading is Mode 1 or by both defining an effective applied stress intensity factor $K_{eff}(K_1,K_2,K_3)$, where $K_{eff} = K_{1c}$ at brittle fracture, and by using an appropriate collapse expression.

This paper addresses crack growth under mixed Modes 1 and 2 small scale yielding conditions. Failure is assumed to coincide with initiation of crack growth. Large-deformation analysis is described in which the details of the stress and strain fields ahead of the blunting crack tip are discerned. Using this analysis, predictive fracture models are discussed. In particular, fracture loci in stress intensity factor space are

* Nuclear Electric, Berkeley Nuclear Laboratories
+ Now at National Power, Swindon

established. A definition of K_{eff} is then derived from the lower bound of the fracture loci and tested against failure data using the R6 method.

STRESS ANALYSIS

Rice and Johnson (2) showed, in Mode 1, that the large strains required in ductile failure models are achieved in a region of the order of the COD in size, when blunting of the crack tip is considered. Budden (3,4) extended this work to mixed Modes 1 and 2 and performed slip-line field analyses which enabled the details of the stress and strain distributions in this intensely strained 'blunting' region near the notch tip to be established. Furthermore, Budden (4) and Budden and Jones (5) evaluated the 'damage' functional

$$D = \int \exp(3\sigma_m/2\sigma_{eq})d\varepsilon_p \qquad (1)$$

in the blunting zone. The integrand of equation (1) has been shown by Rice and Tracey (6) to approximately describe void growth. The stress, strain and damage fields in the blunting zone were then used (5) to derive predictive fracture models.

CLEAVAGE FRACTURE

Shih (7) showed that the stress field ahead of a sharp crack in mixed Modes 1 and 2 is of HRR type (8). Specifically, for a uniaxial power-law material, $\varepsilon_p \propto (\sigma/\sigma_0)^n$, it was shown that

$$\sigma_{ij} = \sigma_0 K_M r^{-1/(n+1)} \tilde{\sigma}_{ij}(\theta; K_1/K_2, n) \qquad (2)$$

Shih also derived the stress field in the limit of perfect plasticity; this formed the boundary condition for the analysis of (3,4).

Ritchie et al (9) argued that cleavage fracture occurs when the fracture stress, σ_f, is achieved over some microstructurally significant length scale, r_c. This model was used (5) to derive failure loci under mixed Modes 1 and 2. From equation (2), the maximum value of the circumferential stress is achieved at $\theta = \bar{\theta}$, say. Equating this maximum to σ_f at $r = r_c$, it can be shown (5) that:

$$(K_1/K_{1c})^2 + (K_2/K_{1c})^2 = \Sigma^{-(n+1)} \qquad (3)$$

where, with $K_1^2 + K_2^2$ fixed,

$$\Sigma = \lim_{r\to 0} \frac{\sigma_\theta(r,\bar{\theta};K_1,K_2)}{\sigma_\theta(r,0;K_1,0)} . \qquad (4)$$

The loci of equation (3) move further from the origin in $(K_2/K_{1c}, K_1/K_{1c})$ space as n increases, with the n = 1 locus providing a lower bound.

The local stress field is perturbed by the effects of blunting. The analysis (3,4) predicts a rise in stress on moving away from the notch tip, the blunting stress field matching onto the sharp crack field at a distance of the order of the COD from the tip. The maximum stress is bounded. For cleavage fracture to occur this maximum must exceed σ_f. In that case, equating equation (2) to σ_f will underestimate the fracture load since it ignores the rising part of the stress curve. It is argued in (5) that equation (3) can then provide a good approximation to the fracture locus when blunting is considered.

It was shown (5) that the maximum stress is bounded by some multiple, k say, of σ_0. Hence cleavage fracture can only occur if $\sigma_0 \geq \sigma_f/k$. σ_0 increases in general as temperature decreases. Hence there can exist a temperature below which cleavage fracture is possible for all K_2/K_1 and a temperature above which cleavage fracture cannot occur. k in general decreases as K_2/K_1 increases (5). Hence at a given temperature a transition can occur from the cleavage micromechanism as K_2/K_1 increases.

DUCTILE FRACTURE

The details are given in (5). The model (6) of void growth was used in conjunction with the analysis of Budden (3,4) to evaluate equation (1) in the blunting zone. The ratio of current to initial void radius is a function of D. Fracture occurs when $D \geq D_{crit}$, a material parameter, over a material dependent distance which is related to the spacing of void nucleating particles. This corresponds to assuming fracture occurs at a critical volume fraction of voids. It was shown in (5) that material-dependent fracture loci were given by

$$(K_1/K_{1c})^2 + (K_2/K_{1c})^2 = h^2(K_1/K_2, D_{crit}) \qquad (5)$$

Approximate expressions for h were given. As D_{crit} increased, h increased and the failure loci moved away from the origin, that is to larger load levels. Comparison with some Mode 1 failure data showed (5) that the method gave conservative predictions of fracture load. A lower bound fracture locus was also given which bounded all the material-dependent loci.

THE EFFECTIVE STRESS INTENSITY FACTOR

For practical failure assessments, a mechanism- and material-independent fracture locus is desirable. The n = 1 cleavage fracture locus is a lower bound to the various loci derived for both failure micro-mechanisms except for a range of K_2/K_1 near

Mode 2 where the material-independent ductile locus is the lower (5). Hence if $\tilde{r} = \tilde{r}(K_1/K_2)$ is the distance of the n = 1 locus from the origin in $(K_2/K_{1c}, K_1/K_{1c})$ space, then a definition of K_{eff} is

$$K_{eff} = (K_1^2 + K_2^2)^{1/2}/\tilde{r} \qquad (6)$$

This bounds above the alternative specific definitions, and is hence conservative, for $K_2 < 2.15K_1$ (5). For $K_2 > 2.15K_1$, K_{eff} can be closely defined by $K_{eff} = K_2/0.7$ (5).

COMPARISON WITH DATA

The general definition of K_{eff}, equation (6), was tested (5) against various failure data obtained from the literature, using the R6 method (1). Figures 1 and 2 shows the result. The data are plotted on R6 Failure Assessment Diagrams. It should be noted that all the data are for low-toughness, high-strength alloys. Moreover most of the ductile data are for aluminium alloys which failed by a strain-controlled mechanism, but not demonstrably one of stable void growth and linkage. It can be seen that most of the data lie outside the R6 Failure Assessment Curve and are therefore consistent with the failure avoidance approach of R6. Further data are however required to fully validate the approach.

ACKNOWLEDGEMENT

This work was performed at Berkeley Nuclear Laboratories and is published with the permission of Nuclear Electric plc.

SYMBOLS USED

h = dimensionless function in equation (5)

k = maximum stress factor

n = stress index

$\tilde{r}$ = dimensionless function in equation (6)

r_c = critical distance

r, θ = polar coordinates

D = damage

D_{crit} = critical damage

K_{eff} = effective stress intensity factor

K_M = amplitude factor in stress field

ε_p = plastic strain

$d\varepsilon_p$ = equivalent plastic strain increment

σ_m = mean stress

σ_{eq} = equivalent stress

σ_0 = yield stress

σ_f = fracture stresses

σ_{ij} = stress tensor

$\tilde{\sigma}_{ij}$ = dimensionless stress tensor

$\bar{\theta}$ = maximum stress angle

Σ = dimensionless function in equations (3), (4)

REFERENCES

(1) Milne,I., Ainsworth,R.A., Dowling,A.R. and Stewart,A.T., Intnl. J. Press. Vessel and Piping, 32, 3-196, 1988.

(2) Rice,J.R. and Johnson,M.A.,"Inelastic Behaviour of Solids", ed. Kanninen, M.F., McGraw-Hill (New York), 1970.

(3) Budden,P.J., J. Mech. Phys. Solids, 35(4), 457-478, 1987.

(4) Budden,P.J., J. Mech. Phys. Solids, 36(5), 503-518, 1988.

(5) Budden,P.J. and Jones,M.R., "Mixed Mode Fracture", CEGB Report RD/B/6159/R89, 1989.

(6) Rice,J.R. and Tracey,D.M., J. Mech. Phys. Solids, 17, 201-217, 1969.

(7) Shih,C.F., "Fracture Analysis", 187-210, ASTM STP 560, 1974.

(8) Hutchinson,J.W., J. Mech. Phys. Solids, 16, 337-347, 1968.

(9) Ritchie,R.O., Knott,J.F. and Rice,J.R., J. Mech. Phys. Solids, 21, 395-410, 1973.

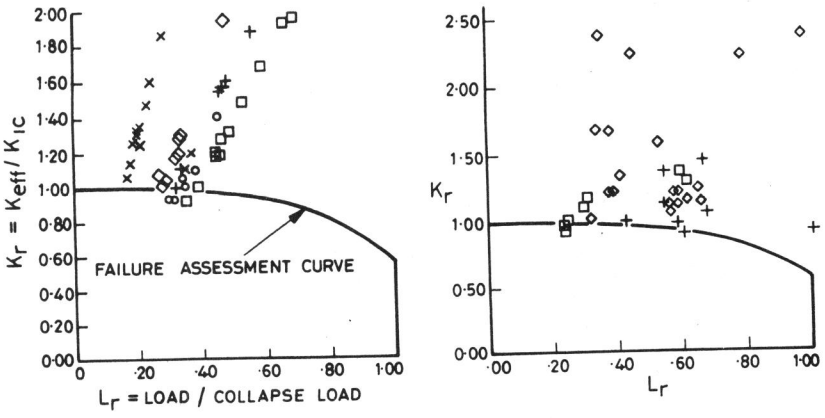

Figure 1. Mixed mode cleavage data

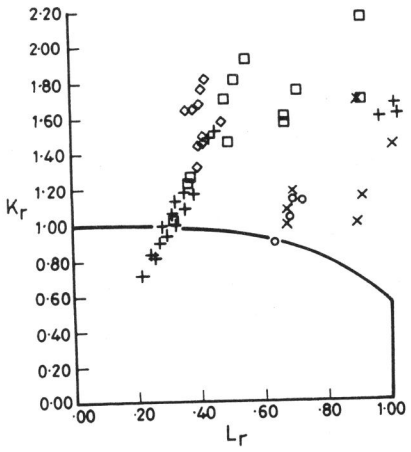

Figure 2. Mixed mode ductile data